

ARTICLE

Open Access

Ceramide synthase-6 confers resistance to chemotherapy by binding to CD95/Fas in T-cell acute lymphoblastic leukemia

Dattesh Verlekar^{1,2,3}, Sung-Jen Wei^{1,2}, Hwangeui Cho^{1,2}, Shengping Yang^{1,4} and Min H. Kang^{1,2,5}

Abstract

Ceramide synthases (CERS) produce ceramides which are key intermediators in the biosynthesis of complex sphingolipids and play an important role in cell proliferation, differentiation, apoptosis and senescence. CERS6 is an isoform of ceramide synthases known to generate ceramides with C16 acyl chain (C₁₆-Cer). CERS6 and C₁₆-Cer levels were significantly higher in acute lymphoblastic leukemia (ALL) cells in comparison to peripheral blood mononuclear cells and T lymphocytes derived from healthy human volunteers. We investigated the role of CERS6 in chemoresistance in T-ALL cell lines. Stable knockdown of *CERS6* in CCRF-CEM and MOLT-4 cells resulted in increased sensitivity to ABT-737, a pan-BCL-2 inhibitor, while CCRF-CEM cells with exogenous *CERS6* expression showed resistance to ABT-737 relative to the vector control. The cytotoxic activity of ABT-737 in *CERS6* knockdown cells was significantly reduced by the addition of a caspase-8 inhibitor Z-IETD, suggesting that CERS6 alters the cytotoxicity via extrinsic pathway of apoptosis. By co-immunoprecipitation of CERS6 in CCRF-CEM cells, we identified CD95/Fas, a mediator of extrinsic apoptotic pathway, as a novel CERS6 binding partner. In Fas pull-down samples, FADD (Fas-associated protein with death domain) was detected at higher levels in cells with *CERS6* knockdown compared with control cells when treated with ABT-737, and this was reversed by the overexpression of *CERS6*, demonstrating that CERS6 interferes with Fas-FADD DISC assembly. CERS6 may serve as a biomarker in determining the effectiveness of anticancer agents acting via the extrinsic pathway in T-ALL.

Introduction

Acute lymphoblastic leukemia (ALL) is the most common childhood and adolescent cancer, and approximately 2900 new cases of pediatric ALL are diagnosed annually in the United States¹. Sixty percent of the cases occur at less than 20 years² and the survival rate of childhood ALL is close to 90%^{3,4}. Although much progress has been made in understanding cellular responses to standard chemotherapeutic agents, approximately 10% of pediatric patients with ALL do not respond to treatment, and

ultimately die of the disease^{3,4}. As cancer cells continue to evolve mechanisms to circumvent stressors leading to development of intrinsic or acquired drug resistance, a significant percentage of patients with standard-risk and high-risk ALL relapse, and post-relapse treatment rarely results in long-term survival⁵. Mortality in high-risk disease is about 35%⁶ and the treatment of infants and adults still needs improvement⁴.

Sphingolipids are bioactive lipids and primarily include sphingosines, ceramides and sphingomyelins that control a variety of cellular functions⁷. Many chemotherapeutic drugs are reported to modulate sphingolipid pathways, though their contribution to cytotoxicity is controversial. Ceramides, key intermediates in the biosynthesis of all the complex sphingolipids, have a significant role in the regulation of cell growth, differentiation, apoptosis and

Correspondence: Min H. Kang (min.kang@ttuhsc.edu)

¹Cancer Center, School of Medicine, Texas Tech University Health Sciences Center, Lubbock, TX 79430, USA

²Department of Pediatrics, School of Medicine, Texas Tech University Health Sciences Center, Lubbock, TX 79430, USA

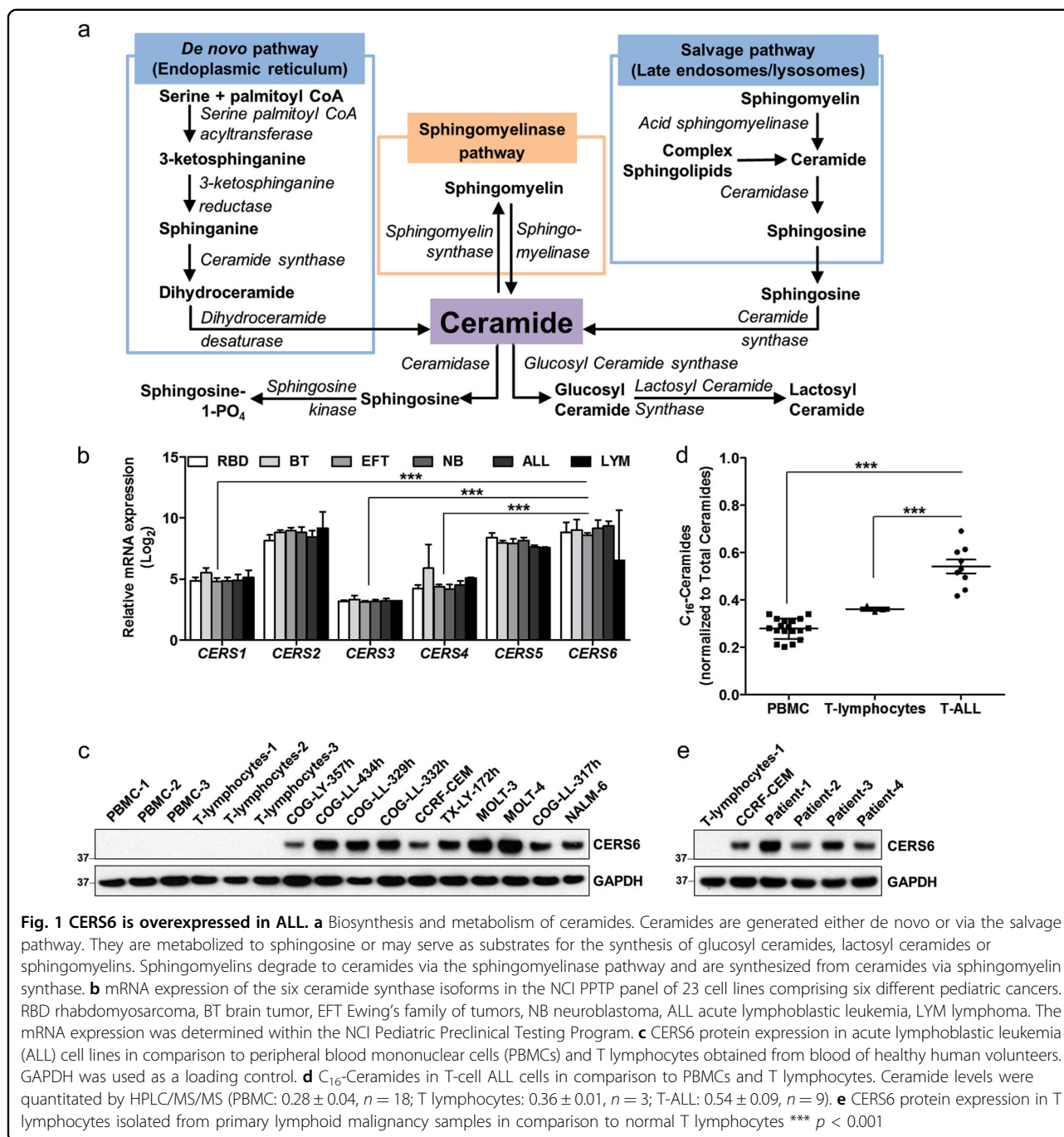
Full list of author information is available at the end of the article.

Edited by M. Herold

© The Author(s) 2018



Open Access This article is licensed under a Creative Commons Attribution 4.0 International License, which permits use, sharing, adaptation, distribution and reproduction in any medium or format, as long as you give appropriate credit to the original author(s) and the source, provide a link to the Creative Commons license, and indicate if changes were made. The images or other third party material in this article are included in the article's Creative Commons license, unless indicated otherwise in a credit line to the material. If material is not included in the article's Creative Commons license and your intended use is not permitted by statutory regulation or exceeds the permitted use, you will need to obtain permission directly from the copyright holder. To view a copy of this license, visit <http://creativecommons.org/licenses/by/4.0/>.



senescence⁸. Six mammalian ceramide synthase (*CERS1*–*6*) homologs use a relatively restricted subset of acyl-Coenzyme A for ceramide synthesis by N-acylation of the sphingoid base⁹. *CERSs* produce ceramides using either the de novo synthesized sphinganine¹⁰ or by acylation of sphingosines from the salvage pathway (Fig. 1a). Ceramides are also generated by breakdown of sphingomyelins using sphingomyelinases.

The expression levels of *CERSs* vary between different tissues. *CERS1* is predominantly expressed in the brain

and skeletal muscles in mouse¹¹. While *CERS2* is ubiquitously expressed, kidney, liver and intestine are the major tissues with high *CERS2* expression¹¹. *CERS3* shows highest expression in testis and *CERS4* is not specific to any particular tissue. *CERS5* has been extensively studied and is the main *CERS* found in the lung epithelia⁷. *CERS6* is expressed in almost all tissues, but shows a very low expression profile in each of them, except for small intestine¹¹. *CERS6* predominantly synthesizes C₁₆-ceramide (C₁₆-Cer) and is subcellularly

localized mainly in the endoplasmic reticulum¹², and also in the plasma membrane¹³. *CERS6* displays homology with *CERS5*¹⁴ and *CERS6* knockout mouse shows a high reduction in C₁₆-Cer levels in most tissues¹⁵. Knockdown of *CERS6* in colon adenocarcinoma cells caused a decrease in C₁₆-Cer and protected the cells against tumor necrosis factor-related apoptosis-inducing ligand (TRAIL)¹⁶, whereas C₁₆-Cer generated by *CERS6* in human head and neck squamous cell carcinoma (HNSCC) cells increased tumor development and growth¹⁷, suggesting an anti-apoptotic role of *CERS6* in tumor cells.

Treatment of pediatric ALL includes remission induction therapy for 4–5 weeks, consolidation therapy for 4–8 weeks, delayed intensification therapy for 8–9 weeks sandwiched between two interim maintenance therapies for 8 weeks each, followed by maintenance therapy for 2–3 years, and is the longest phase of treatment^{18,19}. Glucocorticoid is one of the backbone regimen for the treatment of pediatric ALL. ABT-737 is a small molecule inhibitor of B-cell lymphoma 2 (BCL-2) family of proteins²⁰, which binds directly to the hydrophobic groove of anti-apoptotic BCL-2, B-cell lymphoma-extra large (BCL-X_L) or BCL-w promoting the oligomerization of BAX and BAK to induce apoptosis²¹. Although ABT-737 as a single agent has shown substantial activity in multiple myeloma²², it can significantly enhance the activity of ALL standard-of-care treatment drugs like vincristine, L-asparaginase and dexamethasone in vitro and in vivo²³. A recently developed modified BCL-2 inhibitor, ABT-199, shows high selectivity towards BCL-2 without inhibiting BCL-X_L or BCL-w and is currently approved for chronic lymphocytic leukemia.

The purpose of this study is to understand the roles of ceramides in cancer and to define sphingolipids as potential targets in cancer chemotherapy. We hypothesized that high levels of *CERS6* interfere with apoptosis and render ALL cells resistant to drug treatment. *CERS6* knockdown increased T-ALL cell sensitivity to ABT-737, while *CERS6* overexpression rendered the cells resistant to ABT-737. Finally, we studied whether *CERS6* binds to CD95/Fas and interferes with association of FADD to Fas, and thus inhibiting the extrinsic apoptotic pathway upon drug treatment.

Materials and methods

Chemicals and reagents

Sphingolipid standards including C14:0-, C16:0-, C17:0-, C18:0-, C18:1-, C20:0-, C24:0-, C24:1-ceramide and C18:0-, C18:1-, C24:0-, C24:1-dihydroceramide were purchased from Avanti Polar Lipids (Alabaster, AL); ammonium formate and formic acid were obtained from Fisher Scientific (Pittsburg, PA); chloroform, ethyl acetate, methanol, 2-propanol, NaF, NaHCO₃, Na₃VO₄, Tris-HCl,

Triton X-100, pepstatin A, aprotinin, leupeptin, 200 proof ethanol, isopropanol, puromycin, dexamethasone, and anti-FLAG-M2 (1 µg/ml) antibody from Sigma-Aldrich (St. Louis, MO); ABT-737 from Cayman Chemical (Ann Arbor, MI); DTT, EDTA, NaCl, PMSF, SDS, TBE, trypsin/EDTA, Lipofectamine®, PLUSTM reagent, Superscript® III first-strand synthesis system for RT-PCR from Thermo Fisher Scientific (Waltham, MA); Triton X-114 from Acros Organics (Morris, NJ); Z-IETD from R&D Systems (Minneapolis, MN); Fas ligand from GeneTex (Irvine, CA); anti-*CERS6*, anti-FLIP and anti-GAPDH antibodies from Santa Cruz Biotechnology (Santa Cruz, CA); anti-Fas and anti-FADD from BD Transduction Laboratories (San Jose, CA); anti-HA antibody from Roche (Indianapolis, IN); anti-caspase-3, anti-cleaved-caspase-3, anti-caspase-8 and anti-PARP from Cell Signaling Technology (Danvers, MA); *Age1*-HF, *BamH1*-HF, *EcoR1*-HF, *Mlu1*-HF, *Pme1* and *Sgf1* restriction enzymes from New England Biolabs (Ipswich, MA); bovine serum albumin from Jackson ImmunoResearch Laboratories (West Grove, PA); all oligos were synthesized from Integrated DNA Technologies (Coralville, IA).

mRNA expression of *CERS* isoforms in various cancers

The expression of messenger RNA (mRNA) in the NCI PPTP cell lines were determined in the previous study using Affymetrix U133 Microarray system²⁴. The data were used to determine mRNA expression of *CERS1-CERS6*. *CERS6* expression levels in various cancers and normal tissue samples were obtained from UCSC Xena (<https://xenabrowser.net>)

Extraction of PBMCs and T lymphocytes

Human blood from normal healthy volunteers was obtained from United Blood Services (Lubbock TX). Peripheral blood mononuclear cells (PBMCs) were extracted using LSM-Lymphocyte Separation Medium (MP Biomedicals, Santa Ana, CA) as per the manufacturer's protocol. T lymphocytes were separated from PBMCs using Dynabeads Untouched Human T Cells (Thermo Fisher Scientific, Baltics UAB) extraction kit following the manufacturer's protocol.

Cell culture

ALL cell lines (Supplemental Table S1) used in the study were cultured in RPMI (GE Lifesciences) supplemented with 10% heat-inactivated fetal bovine serum (FBS, Life Technologies) or Iscove's modified Dulbecco's medium (Life Technologies) with insulin–transferrin–selenium (Sigma-Aldrich) (10 µg/ml insulin, 5.5 µg/ml transferrin (substantially iron-free), 5 ng/ml sodium selenite), and 20% heat-inactivated FBS. All cell lines were cultured in physical hypoxia (5% CO₂, and 5% O₂). Cell lines were tested for and free of mycoplasma, and cell line identities were

verified using short tandem repeat genotyping as compared with the original primary sample material within COGcell database: www.COGcell.org.

T lymphocytes from primary clinical samples

Ficoll-separated mononuclear cells from peripheral blood of patients diagnosed with lymphoid malignancies were obtained from the Texas Cancer Cell Repository (TXCCR) with informed consent from all patients. T lymphocytes were separated using Dynabeads Untouched Human T Cells (Thermo fisher Scientific, Baltics UAB) extraction kit following the manufacturer's protocol.

Immunoblotting

Cells grown in T75 or T150 flask were washed once with ice-cold 1× phosphate-buffered saline (PBS). Cells lysis was performed on ice with modified RIPA buffer (50 mM Tris-HCl, pH 7.4, 150 mM NaCl, 1 mM EDTA, 1% Triton X-100 (Triton X-114 for co-immunoprecipitation), 1 µg/ml Leupeptin, 1 µg/ml aprotinin, 1 µg/ml pepstatin A, 1 mM PMSF, 1 mM Na₃VO₄ and 1 mM NaF), followed by centrifugation at 14,000 × *g* for 15 min at 4 °C. Protein concentration was determined by BCA assay (Pierce, Rockford, IL). Equal amount of protein samples were loaded and electrophoretically separated on a 4–12% sodium dodecyl sulfate–polyacrylamide gel electrophoresis (SDS–PAGE), transferred to Hybond membrane (GE Healthcare, Piscataway, NJ), blocked with 1% bovine serum albumin or 5% skim milk, immunoblotted with the indicated primary antibodies and incubated with 1:3000 horseradish peroxidase-conjugated mouse or rabbit immunoglobulin G (IgG) secondary antibodies followed by detection with enhanced chemiluminescence (GE Healthcare). The membrane was stripped and re-probed with anti-GAPDH antibody to confirm equal loading.

Determination of ceramides by LC-MS/MS

The sphingolipids were analyzed using previously reported method²⁵ with modification. Briefly, cell pellet (7.5 × 10⁶ cells) added with 50 µl of internal standard (C17:0-ceramide, 1 pM) was extracted twice with ethyl acetate/2-propanol/water (60/28/12; v/v/v). Sphingolipids were separated using gradient elution with mobile phase A (2 mM ammonium formate and 0.2% formic acid (v/v) in water) and B (1 mM ammonium formate and 0.2% formic acid (v/v) in methanol) on an Agilent 1200 series high-performance liquid chromatography (HPLC) system with Spectra C8SR column (3 µm, 150 × 3.0 mm, Peeke Scientific, Redwood, CA). Mass spectrometric detection was performed by multiple reaction monitoring (MRM) mode on a Sciex 4000 QTRAP mass spectrometer (AB Sciex, Framingham, MA) operating in positive ion mode. Analyst software 1.6.3 (AB Sciex) was used for the data acquisition as well as processing. Sphingolipid data

generated from liquid chromatography-tandem mass spectrometry (LC-MS/MS) were normalized to lipid phosphate as previously described²⁶.

CERS6 knockdown by lentiviral transduction

CERS6 short hairpin RNA (shRNA; TRCN0000128836) in pLKO.1-puro lentiviral vector was from Dharmacon (GE Healthcare Bio-Sciences, Pittsburgh, PA). *pLKO.1-puro eGFP* shRNA sequence (Sigma-Aldrich), which targets enhanced green fluorescent protein (eGFP), was used as a non-targeting control (NT-shRNA). Knockdown of *CERS6* in CCRF-CEM or MOLT-4 cells was carried out as described under “Cell transduction” section below.

Cloning and mutagenesis

CERS6 complementary DNA (cDNA) was amplified by the Expand High Fidelity PCR System (Roche) using pLX304-*CERS6* (DNASU Plasmid Repository, Arizona State University) as a template and primers as specified (Supplemental Table S3). The PCR-amplified *CERS6* gene was subcloned into *SgfI* and *MluI* sites of *pCMV6-Entry-mycDDK* (OriGene, Rockville, MD) to create *pCMV6-CERS6-mycDDK* using LigaFastTM Rapid DNA Ligation System (Promega, Madison WI). *CERS6* was ligated into *EcoRI* and *MluI* sites of pLenti-HTBH-DDK^{27,28} (a kind gift from Dr. Lan Huang, UC Davis, and modified by S-JW) to be used for *CERS6* overexpression by lentiviral transduction. *FAS* cDNA was synthesized using RNA extracted from CCRF-CEM cells and amplified as mentioned above. *FAS* gene was subcloned into *SgfI* and *MluI* sites of *pCMV6-AC-HA* (OriGene, Rockville, MD) to create *pCMV6-AC-FAS-HA*. The *FAS* mutant clones of deletion and point substitutions were generated with specific primers (Supplemental Table S3) using QuikChange Site-Directed Mutagenesis Kit (Agilent, Clara, CA). The DNA sequences of all constructs were verified by MacroGen USA (Rockville, MD) using an automated ABI-3730xl DNA Analyzer and ABI *PRISM[®] BigDye[™] Terminator v3.0 Ready Reaction Cycle Sequencing Kit* (Applied Biosystems, Foster City, CA). All plasmid DNAs were prepared using purification kits from Qiagen (Valencia, CA) and were endotoxin-free when used for transfection into mammalian cells.

Cell transduction

HEK293FT (Life Technologies) cells were cultured in Dulbecco's modified Eagle's medium (Thermo Fisher Scientific) supplemented with 10% FBS, 2 mM glutamine, 100 units/ml penicillin, 100 µg/ml streptomycin sulfate and 1 mM sodium pyruvate (Life Technologies). Ten million cells were plated at cell on a 10 cm tissue culture dish and incubated at 37 °C 5% CO₂ incubator until the cells reach 80% confluence. The HEK293FT cells were co-transfected with either lentiviral open reading frames or

shRNAs along with Lenti-vpak Packaging Kit (OriGene) using the transfection reagent MegaTran 1.0 (OriGene). After 48–72 h of transfection, the virus-containing medium was collected, spun down, filtered (0.45 μm) and used for targeting into CCRF-CEM or MOLT-4 cells by infection. The virus-infected stable clones were obtained after at least 2–3 weeks of selection in 10% FBS/RPMI-1640 with 0.5 $\mu\text{g}/\text{ml}$ of puromycin (Sigma-Aldrich).

Cell transfection

HEK293FT cells at 80% confluency were transfected with recombinant DNA constructs (Fig. 6a) along with Plus reagent and Lipofectamine (both from Invitrogen, Carlsbad, CA). Cells were harvested after 48 h of transfection and samples prepared as described under “Immunoblotting” section above.

DIMSCAN cytotoxicity assay

Cells were plated (3000 cells/well for CCRF-CEM and 4500 cells/well for MOLT-4) in a 96-well plate using 150 μl of culture medium and incubated for at least 12 h followed by 50 μl of drug treatment at the following concentrations: 0.001 to 1 μM for ABT-737 and 0.0001 to 1 μM for dexamethasone. Stock solutions for ABT-737 was prepared using dimethyl sulfoxide and dexamethasone was prepared using sterile water. DIMSCAN assay was performed for 72 h post treatment as previously described²⁹.

Apoptosis assay by flow cytometry

Apoptosis was determined using Annexin-V surface positivity by flow cytometry. CCRF-CEM or MOLT-4 cells were incubated with ABT-737, Z-IETD or combination, washed twice with PBS and subjected to Annexin-V assay using Apo AlertTM Annexin-V-FITC Apoptosis kit (Takara Clontech, Mountain View, CA) as previously described²³.

Immunoprecipitation (IP)

The cell lines samples were prepared for IP as indicated in the “Immunoblotting” section. For purification of CERS6 (Fig. 5a), 2000 μg of protein lysates as prepared above were pulled down at 4 °C overnight with Ni-NTA His-Bind Resin (EMD-Millipore, Billerica, MA), washed 4 times with modified RIPA and then eluted with 350 mM imidazole. Further, the eluate was incubated with EZview Red Streptavidin Affinity Gel (Sigma) for 2 h, washed 4 times with modified RIPA, and digested with AcTEV Protease (Invitrogen, Carlsbad, CA) for 3 h. Immunoprecipitation of Fas was performed using 1000 μg of protein lysates incubated with 2 μg of anti-Fas antibody Rb (Proteintech, Rosemont, IL) overnight at 4 °C. Fas and associated proteins were pulled down using 50 μl of Protein G Plus Agarose beads (Santa Cruz Biotechnology,

Santa Cruz, CA) and sample prepared using 4 \times NuPAGE lithium dodecyl sulfate loading buffer and 100 mM DTT, followed by heating at 70 °C for 10 min. For immunoprecipitation of CERS6 (Fig. 6b), 1000 μg of protein lysates were pulled down at 4 °C overnight with 50 μl EZview Red anti-FLAG-M2 affinity gels (Sigma-Aldrich), washed 4 times with modified RIPA and then eluted with an excess of 3 \times FLAG peptide (100 $\mu\text{g}/\text{ml}$). Immuno-complexes were resolved by 4–12% SDS-PAGE and immunoblotted with the indicated antibodies.

Cellular fractionation

Cytoplasmic and plasma membrane fractions were isolated from 293FT whole cells using MinuteTM Plasma Membrane Protein Isolation and Cell Fractionation Kit (Invent Biotechnologies, Plymouth, MN) as specified by the manufacturer's protocol.

FAS surface expression

FAS expression levels were determined in CERS6 knockdown and overexpressing CCRF-CEM cells by flow cytometry using CD95-FITC and FITC Mouse Anti-human IgG (both from BD Biosciences, San Jose, CA) as described previously³⁰. Briefly, cells at logarithmic growth phase were washed twice with PBS, and resuspended in 100 μl of binding buffer (BD Biosciences) at a final concentration of 0.5×10^6 cells per 50 μl . Either anti-human IgG-FITC or CD95-FITC (20 μl per sample) was added to the cell suspension, and the mixture was incubated for 10 min at room temperature. The cells were washed and resuspended in 390 μl of binding buffer. The cells were analyzed by flow cytometry (BD LSR II operated by FACS DIVA) with band-pass filters of 525 ± 25 nm.

Statistical analysis

Assessment of significance were performed using Student's *t*-test and test results were considered significant at $p < 0.05$. Data were plotted and analyzed using GraphPad Prism 6 and SigmaPlot v11.

Results

CERS6 is highly expressed in T-ALL cells in comparison to normal cells

The mRNA expression of six CERS isoforms was analyzed in the NCI PPTP (National Cancer Institute Pediatric Preclinical Testing Program) panel of 23 cell lines²⁹. *CERS2*, *CERS5* and *CERS6* expression levels were significantly higher than *CERS1*, *CERS3* and *CERS4* (8.7 ± 0.4 , 7.9 ± 0.3 and 8.6 ± 1.0 vs 5.0 ± 0.3 , 3.2 ± 0.1 and 4.7 ± 0.7 , $p < 0.0001$, Fig. 1b). Moreover, the relative expression was consistent (CV for *CERS1*: 5.6%, *CERS2*: 4.2%, *CERS3*: 2.2%, *CERS4*: 14.1%, *CERS5*: 3.9% and *CERS6*: 12.1%) in all the 23 cell lines analyzed, but different from the tissue distribution in normal cells¹¹. *CERS2* has been reported to

be the most abundant enzyme with highest expression in most tissues, while mRNA expression of *CERS6* is low in major tissues¹¹. Here, we observed that the levels of *CERS6*, responsible for the generation of C_{16} -Cer, were as high in cancer cells and similar to the levels of *CERS2* (8.7 ± 0.4) among all cell lines tested. *CERS6* was also found to be overexpressed in several other adult cancers when compared to normal tissue samples (Supplemental Fig. S1).

Next, we compared *CERS6* protein levels in 10 leukemia cell lines (Supplemental Table S1)³¹ to PBMCs and T lymphocytes isolated from blood of healthy human volunteers, representing normal cells. *CERS6* levels were significantly higher in ALL cells compared to PBMCs or T lymphocytes (Fig. 1c). To verify the functionality of *CERS6*, the levels of C_{16} -Cer, the product of *CERS6*, were quantitated in ALL and normal cells by LC/MS/MS. As anticipated, C_{16} -Cer levels were significantly higher in ALL cell lines in comparison to PBMCs or T lymphocytes (0.54 ± 0.09 vs 0.28 ± 0.04 , $p < 0.001$ or 0.36 ± 0.01 , $p < 0.001$, Fig. 1d). To investigate whether *CERS6* levels are elevated in primary T-lymphoid malignancies, we employed clinical samples from four lymphoid malignancy patients (Supplemental Table S2) and found that the levels of *CERS6* were higher in T lymphocytes isolated from the four patient samples in comparison to normal T lymphocytes (Fig. 1e).

***CERS6* alters sensitivity of ALL cells to ABT-737, a pan-BCL-2 family of protein inhibitor**

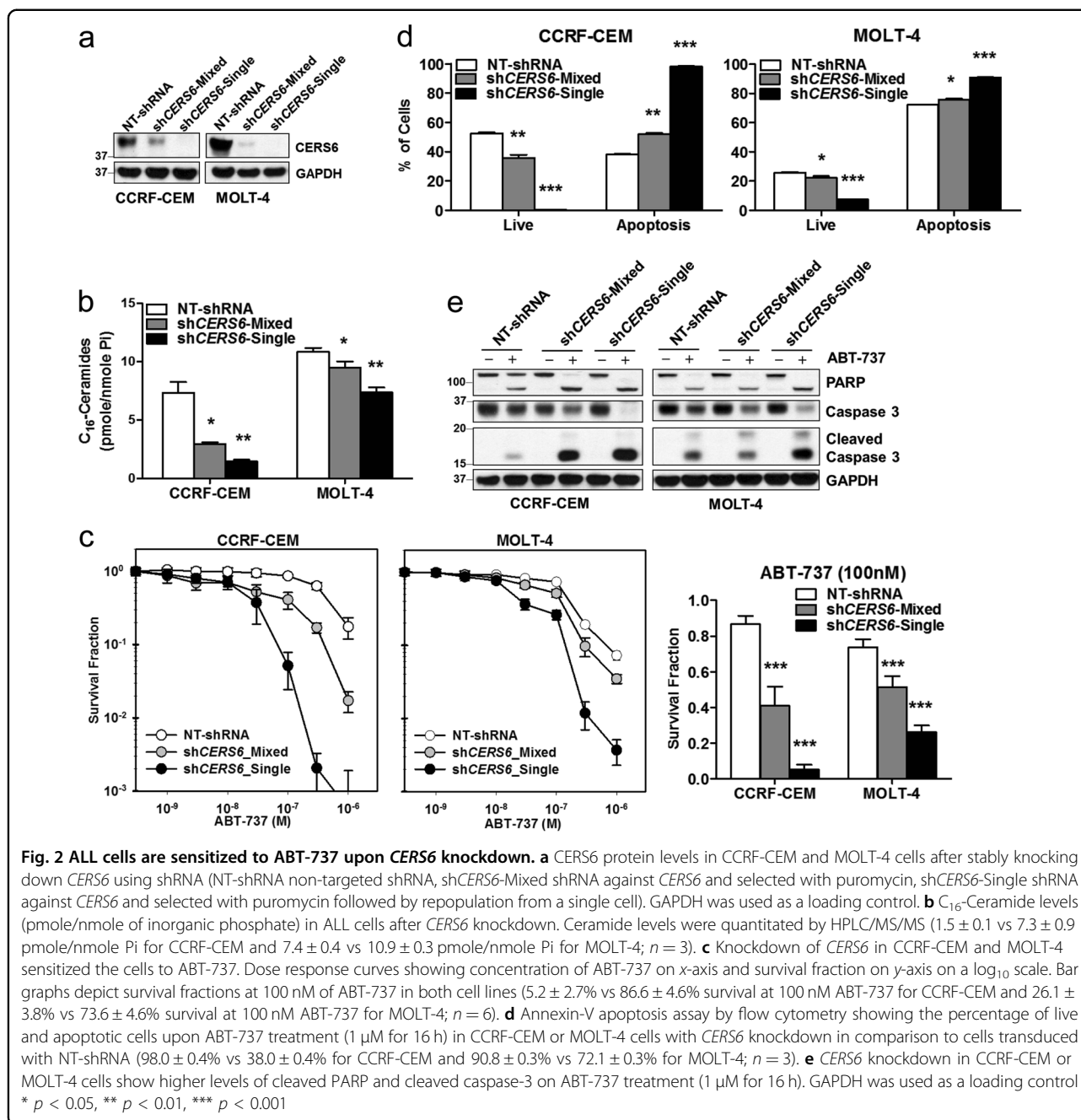
To determine whether higher levels of *CERS6* in ALL contributes to resistance in cytotoxicity of chemotherapeutic drugs, we carried out loss-of-function (knockdown of *CERS6*) and gain-of-function (*CERS6* overexpression) experiments in ALL cells. *CERS6* was stably knocked down using shRNA by lentiviral transduction in two T-ALL cell lines, CCRF-CEM and MOLT-4. The decrease in *CERS6* levels after *CERS6* knockdown was confirmed by immunoblotting (Fig. 2a). C_{16} -Cer levels were significantly reduced in *CERS6* knockdown cells compared with cells transduced with non-targeted shRNA (1.5 ± 0.1 vs 7.3 ± 0.9 pmole/nmole Pi, $p < 0.01$ for CCRF-CEM and 7.4 ± 0.4 vs 10.9 ± 0.3 pmole/nmole Pi, $p < 0.01$ for MOLT-4, Fig. 2b), demonstrating that the *CERS6* activity was also reduced with the decrease in *CERS6* levels in both cell lines. Then, the effect of *CERS6* knockdown on the cytotoxicity of ABT-737, a pan-BCL-2 inhibitor, was evaluated. Both CCRF-CEM and MOLT-4 cells with *CERS6* knockdown displayed a significant increase in cytotoxicity upon ABT-737 treatment ($5.2 \pm 2.7\%$ vs $86.6 \pm 4.6\%$ survival at 100 nM ABT-737, $p < 0.001$ for CCRF-CEM and $26.1 \pm 3.8\%$ vs $73.6 \pm 4.6\%$ survival at 100 nM ABT-737, $p < 0.001$ for MOLT-4, Fig. 2c). In both cell lines with *CERS6* knockdown, the percentage of

apoptotic cells in response to ABT-737 treatment was significantly higher compared with the cells transduced with non-targeted shRNA ($98.0 \pm 0.4\%$ vs $38.0 \pm 0.4\%$, $p < 0.0001$ for CCRF-CEM and $90.8 \pm 0.3\%$ vs $72.1 \pm 0.3\%$, $p < 0.0001$ for MOLT-4, Fig. 2d and Supplemental Fig. S2). Immunoblotting showed that cleaved poly (ADP-ribose) polymerase (PARP) and cleaved caspase-3, markers for apoptotic cell death, were increased in both cell lines with *CERS6* knockdown upon ABT-737 treatment in comparison to cells transduced with non-targeted shRNA (Fig. 2e).

Based on the expression of *CERS6* in ALL cells, CCRF-CEM cells with relatively low *CERS6* expression was selected for exogenous expression of *CERS6*. After stably expressing *CERS6* in CCRF-CEM cells, the increase in *CERS6* protein was confirmed in comparison to cells transduced with control vector (Fig. 3a). C_{16} -Cer levels in CCRF-CEM cells with exogenous *CERS6* expression were significantly higher relative to its control cells (10.1 ± 0.5 vs 5.7 ± 0.1 pmole/nmole Pi, $p < 0.001$, Fig. 3b). Increase in *CERS6* levels rendered CCRF-CEM cells resistant to ABT-737 in comparison to control cells ($39.5 \pm 2.2\%$ vs $2.3 \pm 1.8\%$ survival at 300 nM ABT-737, $p < 0.001$, Fig. 3c). The percentage of apoptotic cells were significantly lower ($36.8 \pm 3.8\%$ vs $85.2 \pm 0.6\%$, $p < 0.01$, Fig. 3d), and cleaved PARP and caspase-3 were less (Fig. 3e) in CCRF-CEM cells overexpressing *CERS6* in comparison to cells transduced with control vector when treated with ABT-737.

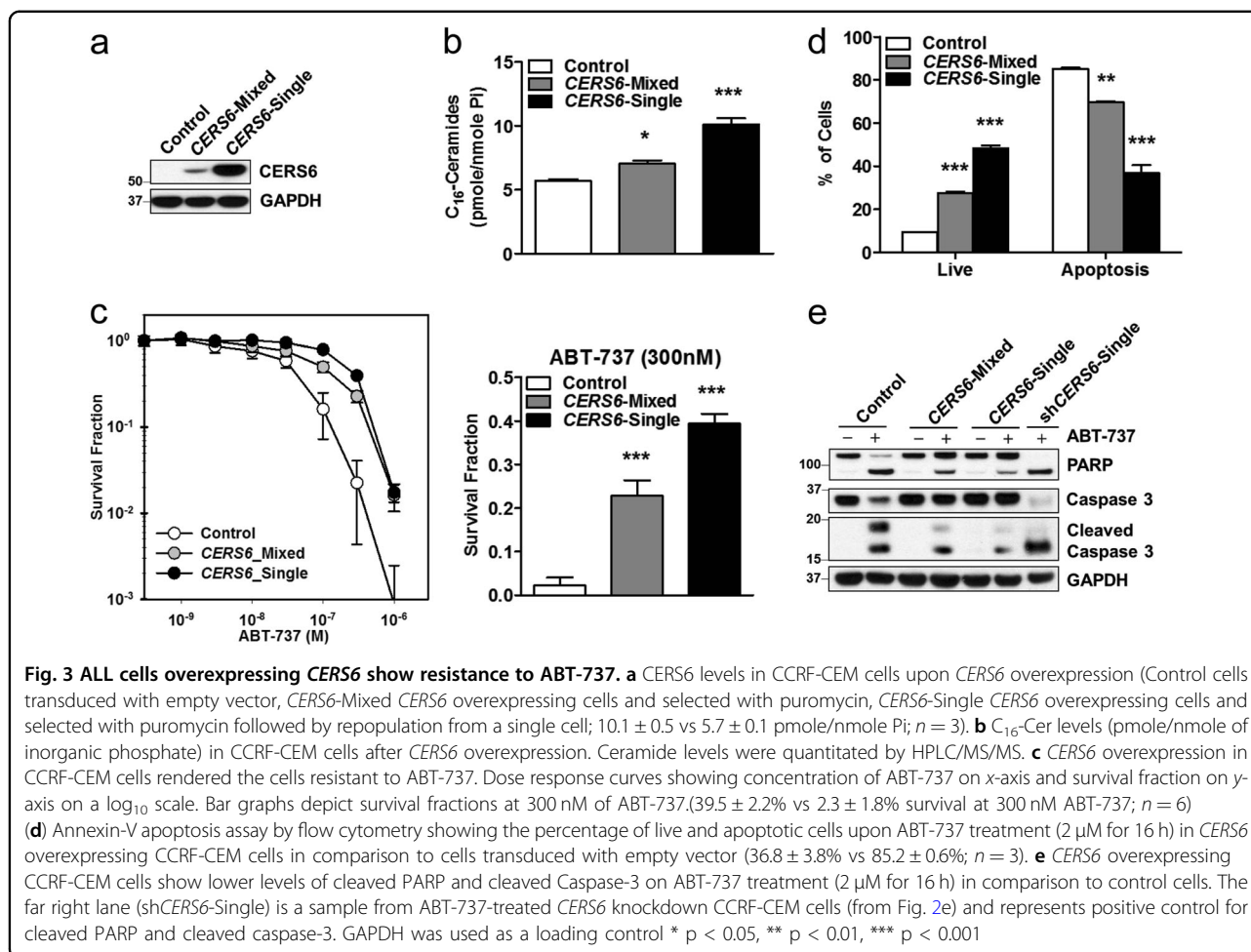
***CERS6*-mediated resistance to ABT-737 occurs via the extrinsic pathway of apoptosis**

ABT-737-inducing apoptosis via mitochondrial (intrinsic) pathway of apoptosis is well documented. However, the extent of changes in anti- and pro-apoptotic BCL-2 family of proteins in ALL cells with *CERS6* knockdown or exogenous expression was not consistent with the differences in cytotoxicity of ABT-737 (Supplemental Fig. S3a). Ceramides in plasma membranes are reported to form “ceramide-enriched platforms” which aid in clustering of death receptors in the extrinsic pathway of apoptosis³². Thus, the effect of *CERS6* modulation in extrinsic apoptotic pathway in response to ABT-737 treatment was investigated. The involvement of extrinsic apoptotic pathway was assessed by measuring the levels of cleaved caspase-8 in CCRF-CEM and MOLT-4 cells with *CERS6* knockdown upon treatment of ABT-737. Higher levels of cleaved caspase-8 were observed in both cell lines with *CERS6* knockdown compared with their respective controls (Fig. 4a), demonstrating that *CERS6* is associated with ABT-737 resistance via the extrinsic pathway of apoptosis. Then, CCRF-CEM and MOLT-4 with *CERS6* knockdown were treated with Z-IETD, a caspase-8 inhibitor, 1 h prior to ABT-737 treatment. The percentage of apoptotic cells was significantly decreased in cells with



CERS6 knockdown pretreated with Z-IETD in response to ABT-737 in comparison to cells without Z-IETD pretreatment ($23.4 \pm 1.7\%$ vs $37.5 \pm 1.5\%$, $p < 0.01$ for CCRF-CEM and $8.2 \pm 0.1\%$ vs $20.8 \pm 0.3\%$, $p < 0.01$ for MOLT-4, Fig. 4b). Cleaved caspase-8, PARP and caspase-3 were reduced by the addition of Z-IETD in *CERS6* knockdown cells treated with ABT-737 compared with cells without the caspase-8 inhibitor (Fig. 4c). We measured changes in soluble Fas ligand (FasL) in culture medium upon treatment of ABT-737 and found that ABT-737 induced the

release of soluble FasL into the medium and that FasL release by ABT-737 was earlier and greater in *CERS6* knockdown cells relative to its empty vector control (Fig. 4d). Further, when CCRF-CEM cells were treated with soluble FasL, cells with *CERS6* knockdown showed significantly higher percentage of apoptotic cells compared with cells transduced with non-targeted shRNA ($70.9 \pm 0.6\%$ vs $14.1 \pm 0.1\%$, $p < 0.0001$, Fig. 4e). CCRF-CEM cells with *CERS6* knockdown were sensitized to dexamethasone, part of ALL standard treatment, in



comparison to control cells ($32.5 \pm 11.9\%$ vs $2.2 \pm 1.1\%$ survival at 100 nM, $p < 0.001$, Supplemental Figs. S3b, c).

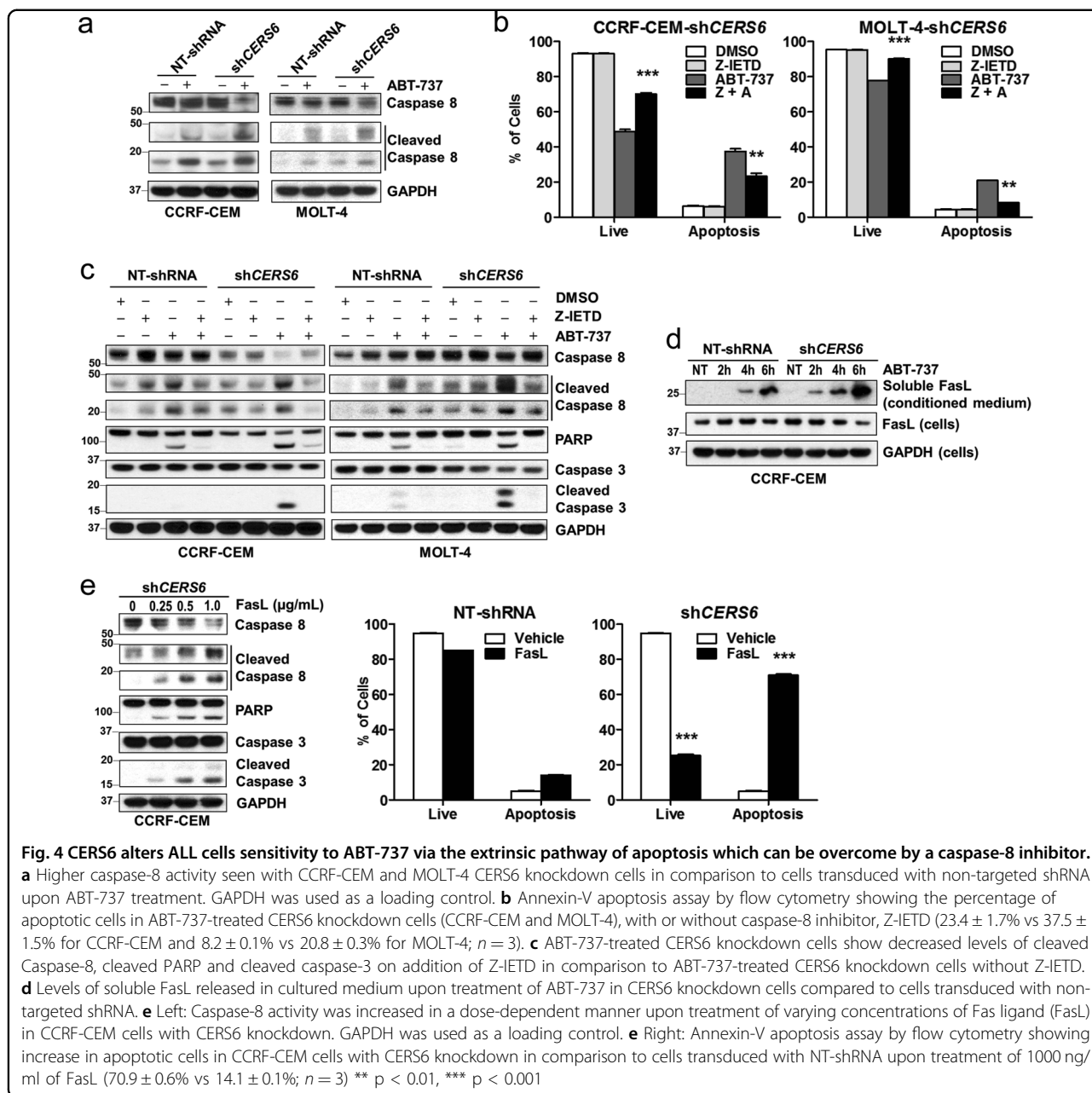
CERS6 binds to CD95/Fas and interferes with FADD assembly to Fas in the extrinsic pathway of apoptosis

After showing that CERS6 interferes with the extrinsic pathway of apoptosis, we sought to determine the mechanism by which caspase-8 activation is attenuated by CERS6. We wanted to see if CERS6 interacted with any of the key players involved in the extrinsic pathway of apoptosis, namely Fas death receptor, FADD (Fas-associated protein with death domain), or caspase-8. Co-immunoprecipitation of CERS6 in CERS6 overexpressing CCRF-CEM cells using a two-step purification protocol (Fig. 5a) was conducted. The efficiency of the pull-down was confirmed by detecting CERS6 at different stages of purification (Fig. 5b). The results showed that CERS6 binds to Fas death receptor, also known as CD95, when the final pull-down sample was probed with Fas antibody (Fig. 5c). Fas ligand binds to Fas death receptor to form the death-inducing signaling complex (DISC) composed of Fas, FADD and pro-caspase-8³³ which initiates caspase-

8 cleavage, further transducing a downstream signaling cascade of caspase activation resulting in apoptosis. Then, Fas was pulled down in ABT-737-treated CCRF-CEM cells to assess the effect of CERS6 on FADD association with Fas. We found that higher levels of FADD were associated with Fas in cells with CERS6 knockdown as compared to control cells on treatment with ABT-737 (Fig. 5d). We also found a decrease in FADD–Fas association in CCRF-CEM cells overexpressing CERS6 on ABT-737 treatment in comparison to ABT-737-treated CCRF-CEM CERS6 knocked down cells (Fig. 5e). Together, these results suggest that CERS6 binds to Fas and inhibits its assembly with FADD leading to decreased apoptosis via the extrinsic pathway.

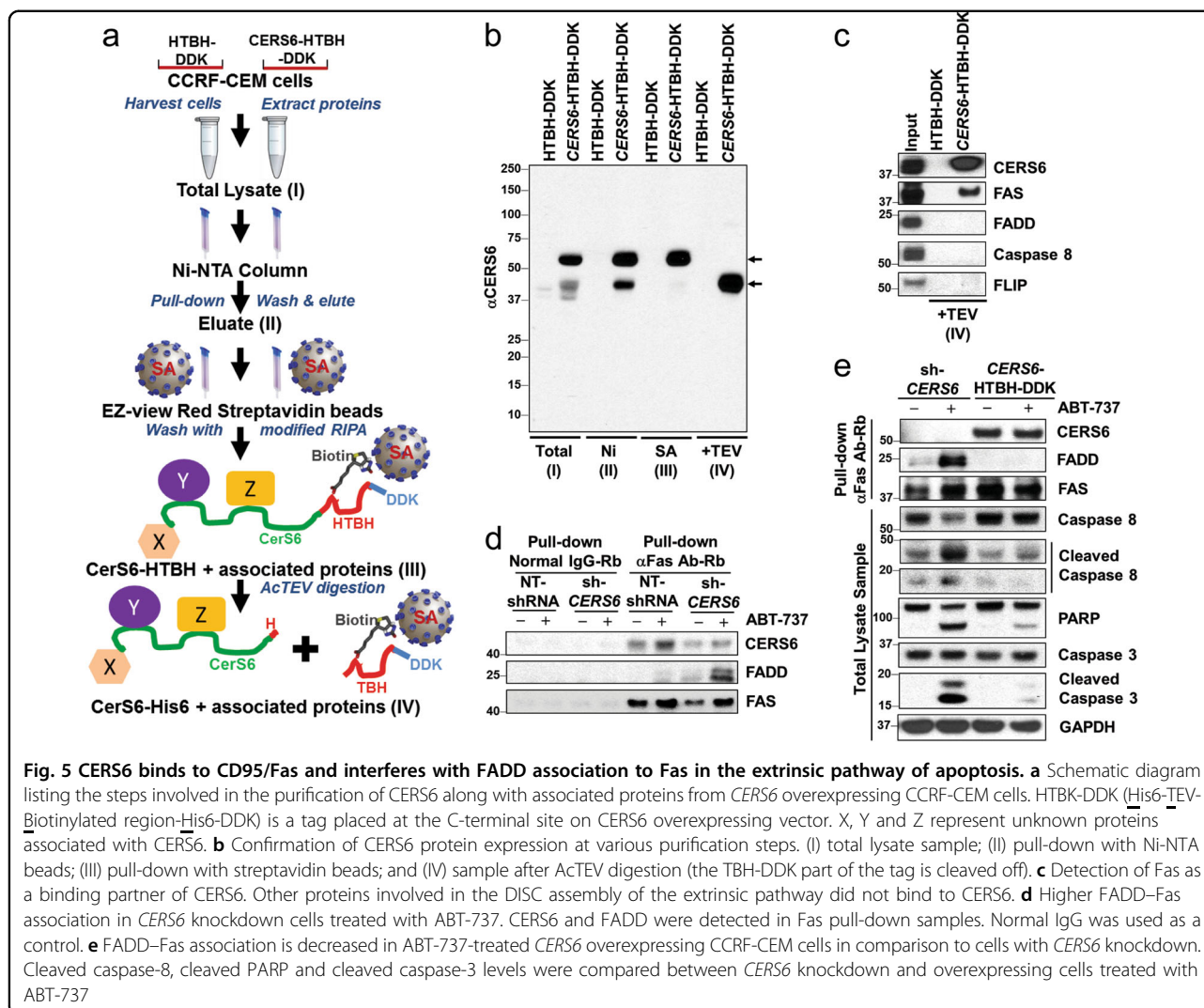
CERS6 binds to intracellular domains of CD95/Fas

In order to determine the binding site of CERS6 on Fas, CERS6 and Fas were exogenously expressed in HEK293FT cells using two distinct tags, CERS6 with mycDDK and Fas with HA tag. To determine if any particular domain was critical for CERS6-Fas binding, deletion mutants of Fas intracellular region were



constructed as shown in Fig. 6a. The binding was anticipated to occur in the death domain, the region where FADD binds to Fas to form DISC³⁴, but, the deletion of the death domain only, did not affect CERS6 binding to Fas (Fig. 6b, left). Cysteine 199 residue adjacent to the transmembrane domain of Fas has been reported to be critical for the ability of Fas to trigger apoptosis³⁵. The binding persisted even with the C199V mutation on Fas, suggesting that this residue is not critical for CERS6 binding to Fas. The binding of CERS6 to each of the deletion mutants in the intracellular region of Fas indicates that CERS6 binding to Fas involves multiple sites of

Fas. To confirm this, deletion mutants (Δ 174–314 and Δ 174–236 and 315–335, Fig. 6a) of the Fas intracellular region were constructed. The binding was lost with the deletion of amino acids 174 to 314, the region comprising the transmembrane domain to death domain, while the deletion of the entire cytoplasmic region except for the death domain did not affect the binding, suggesting that the binding occurs at more than one region from amino acids 174 to 314 (Fig. 6b, right). Further, we also confirmed that the binding of CERS6 and FAS mainly occurs in in plasma membrane relative to cytoplasmic fraction (which includes endoplasmic reticulum (ER) and other



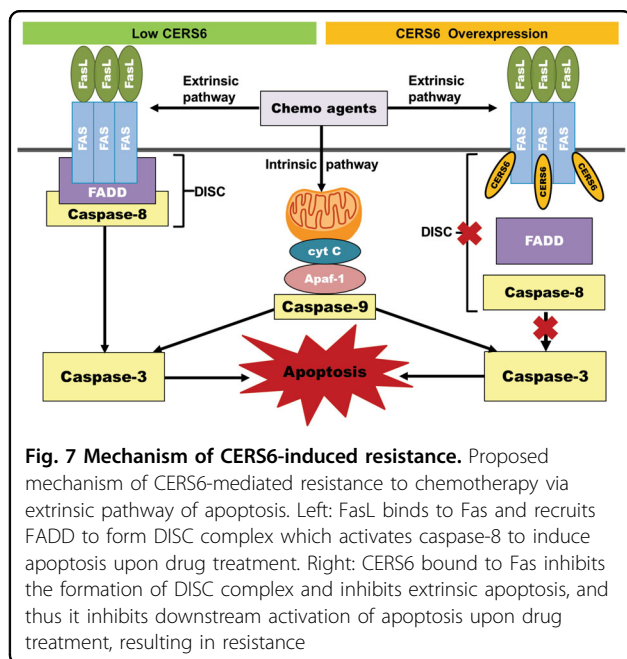
organelles) even with exogenous expression of CERS6 in cytoplasm (Fig. 6c). To conclude, our data show that CERS6 binds to Fas and inhibits the formation of DISC thereby blocking apoptosis upon treatment of drugs acting via extrinsic pathway of apoptosis (Fig. 7).

Discussion

Sphingolipid profiles are frequently altered between cancer cells and normal cells, which may be an indication of prevailing mechanisms used by tumor cells to overcome stressors. Here we report (1) that ceramide synthase-6 (CERS6), an enzyme responsible for the generation of C16 ceramides, is overexpressed in T-cell ALL cells compared with T lymphocytes and PBMCs; (2) that genetic modification of *CERS6* in T-cell ALL cell lines resulted in significant changes in sensitivity to chemotherapeutic drugs; and (3) that CERS6 binds to Fas and renders resistance to chemotherapy via the extrinsic

apoptotic pathway by interfering with the Fas-FADD association in ALL cells.

Several studies have examined how the metabolism of bioactive sphingolipids is reconfigured in cancer and whether modulating the balance between pro-apoptotic and pro-survival sphingolipids can overcome resistance to anticancer drugs¹². For instance, treatment of chemo-resistant chronic myeloid leukemia cells with a BCR-ABL tyrosine kinase inhibitor demonstrated that increase in ceramide synthases preceded cell death³⁶. Treatment of HL-60/VCR, the multidrug-resistant variant of HL-60 leukemia cells, with curcumin induced an increase in ceramide generation and accumulation, leading to apoptosis³⁷. However, a majority of these studies consider ceramide species and corresponding ceramide synthases to be pro-apoptotic, without species-specific differences in activity or the mechanisms of inducing or interfering apoptosis in



Our observation on higher levels of CERS6 and C₁₆-Cer in T-ALL cell lines is consistent with a few other cancers as reported in the literature. C₁₆-Cer levels were significantly higher in breast cancer relative to normal tissues³⁸, while CERS6 mRNA levels were found to be expressively increased in ER-positive tumors in comparison to ER-negative tumors³⁹. In non-small cell lung cancer, *CERS6* levels were markedly higher in comparison to controls and was found to be associated with poor prognosis and increased metastasis⁴⁰. C₁₆-Cer levels were significantly increased in HNSCC which correlated with higher mRNA expression of *CERS6*, when 12 pairs of HNSCC tumors and normal tissues were compared⁴¹. In our study, we have shown higher expression of CERS6 in T-ALL in comparison to normal cells is associated with T-ALL drug resistance.

Previously, it has been shown that knockdown of *CERS6* in HNSCC cells induced stress-mediated apoptosis which could be reversed by overexpressing *CERS6* in these cells¹⁷. We knocked down *CERS6* as well as overexpressed it in ALL cell lines and showed that these genetic alterations changed the sensitivity of ALL cells to chemotherapy. Our studies further demonstrated that CERS6-altered ALL sensitivity to ABT-737 occurs via the extrinsic pathway, by using a caspase-8 inhibitor. Although ABT-737 is anticipated to primarily act via the mitochondrial pathway of apoptosis, it has also been reported to act through the extrinsic pathway, where it enhances TRAIL-mediated cytotoxicity in renal, prostate and lung cancer cells by upregulating TRAIL receptor, death receptor 5⁴².

Our study suggests the expression of CERS6 as the mediator in inducing resistance to chemotherapy acting via extrinsic pathway of apoptosis.

We have demonstrated that there is clear processing of caspase-8 upon ABT-737 treatment, in order to show the involvement of extrinsic apoptotic pathway. However, caspase cleavage during late-stage apoptosis does not faithfully indicate one pathway or another⁴³. To further confirm the involvement of extrinsic pathway, we conducted experiments by treating the cells with FasL, which is exclusive to the extrinsic pathway of apoptosis and showed that caspase-8 is activated in CERS6 knockdown cells (Fig. 4e). In addition, we have studied the effect of knockdown or overexpression of CERS6 on the cell surface expression of FAS. We conducted flow cytometric analysis of FAS cell surface expression in CERS6 knockdown and exogenous expressed cells. Interestingly, CERS6 knockdown resulted in increased FAS cell surface expression (Supplemental Fig. S4). However, CERS6 overexpression did not affect the expression of FAS. The mechanism of FAS increase with the knockdown of CERS6 warrants further investigation in future studies.

Finally, we show that CERS6 binds to Fas and interferes with Fas–FADD association to form DISC complex which activates caspase-8 in the extrinsic pathway of apoptosis. Fas has been reported to interact with a palmitoyl transferase, DHHC7 (aspartate-histidine-histidine-cysteine family of acyl transferases) which stabilizes Fas by palmitoylation at C199³⁵. Being an acyl transferase, CERS6 was thought to interfere with binding of DHHC7 thereby destabilizing Fas and its ability to cause apoptosis. Binding of CERS6 to Fas persisted with C199V mutation, suggesting that C199 is not critical for CERS6 binding. BCL2L13 and SIRT3 are two proteins reported to be interacting with CERS6, where the former is shown to inhibit the activity of CERS6⁴⁴, while the latter deacetylates CERS6 to cause an increase in its activity⁴⁵. These interactions affect the activity of CERS6, but there are no reports showing that CERS6 affects the function of other proteins. Here, we show that CERS6 affects the function of Fas by directly interfering with its assembly with FADD.

In summary, our study shows that CERS6 plays an important role in ALL resistance to chemotherapy by interfering with the Fas–FADD assembly in the extrinsic pathway of apoptosis. CERS6 may serve as a biomarker to stratify ALL patients to determine whether they were likely to respond to drugs acting via the extrinsic pathway of apoptosis. As cancer cells continue to develop resistance to chemotherapeutic drugs and evolve new mechanisms to evade apoptosis, future studies on determining CERS6 as a biomarker for drug resistance in cancer are warranted.

Acknowledgements

This work was funded by the National Cancer Institute, NIH (R15CA159308 to MHK), and by Cancer Prevention and Research Institute of Texas (individual investigator awards RP101042 to MHK). We would like to thank Dr. C. Patrick Reynolds, Director of Cancer Center, TTUHSC and the Cancer Center staff for providing us with clinical samples.

Author details

¹Cancer Center, School of Medicine, Texas Tech University Health Sciences Center, Lubbock, TX 79430, USA. ²Department of Pediatrics, School of Medicine, Texas Tech University Health Sciences Center, Lubbock, TX 79430, USA. ³Department of Cell Biology and Biochemistry, School of Medicine, Texas Tech University Health Sciences Center, Lubbock, TX 79430, USA. ⁴Department of Pathology, School of Medicine, Texas Tech University Health Sciences Center, Lubbock, TX 79430, USA. ⁵Department of Internal Medicine, School of Medicine, Texas Tech University Health Sciences Center, Lubbock, TX 79430, USA

Conflict of interest

The authors declare that they have no conflict of interest.

Publisher's note

Springer Nature remains neutral with regard to jurisdictional claims in published maps and institutional affiliations.

Supplementary Information accompanies this paper at (<https://doi.org/10.1038/s41419-018-0964-4>).

Received: 20 April 2018 Revised: 11 July 2018 Accepted: 25 July 2018

Published online: 11 September 2018

References

- Siegel, R., Naishadham, D. & Jemal, A. Cancer statistics, 2012. *CA Cancer J. Clin.* **62**, 10–29 (2012).
- Pui, C. H., Robison, L. L. & Look, A. T. Acute lymphoblastic leukaemia. *Lancet* **371**, 1030–1043 (2008).
- Hunger, S. P. et al. Improved survival for children and adolescents with acute lymphoblastic leukemia between 1990 and 2005: a report from the Children's Oncology Group. *J. Clin. Oncol.* **30**, 1663–1669 (2012).
- Pieters, R. et al. A treatment protocol for infants younger than 1 year with acute lymphoblastic leukaemia (Interfant-99): an observational study and a multicentre randomised trial. *Lancet* **370**, 240–250 (2007).
- Oriol, A. et al. Outcome after relapse of acute lymphoblastic leukemia in adult patients included in four consecutive risk-adapted trials by the PETHEMA Study Group. *Haematologica* **95**, 589–596 (2010).
- Pui, C. H. et al. Treating childhood acute lymphoblastic leukemia without cranial irradiation. *N. Engl. J. Med.* **360**, 2730–2741 (2009).
- Hannun, Y. A. & Obeid, L. M. Principles of bioactive lipid signalling: lessons from sphingolipids. *Nat. Rev. Mol. Cell Biol.* **9**, 139–150 (2008).
- Ogretmen, B. & Hannun, Y. A. Biologically active sphingolipids in cancer pathogenesis and treatment. *Nat. Rev. Cancer* **4**, 604–616 (2004).
- Mullen, T. D., Hannun, Y. A. & Obeid, L. M. Ceramide synthases at the centre of sphingolipid metabolism and biology. *Biochem. J.* **441**, 789–802 (2012).
- Reynolds, C. P., Maurer, B. J. & Kolesnick, R. N. Ceramide synthesis and metabolism as a target for cancer therapy. *Cancer Lett.* **206**, 169–180 (2004).
- Levy, M. & Futerman, A. H. Mammalian ceramide synthases. *IUBMB Life* **62**, 347–356 (2010).
- Kitatani, K., Taniguchi, M. & Okazaki, T. Role of sphingolipids and metabolizing enzymes in hematological malignancies. *Mol. Cells* **38**, 482–495 (2015).
- Ghosh, D., Lippert, D., Krokhn, O., Cortens, J. P. & Wilkins, J. A. Defining the membrane proteome of NK cells. *J. Mass Spectrom.* **45**, 1–25 (2010).
- Weinmann, A., Galle, P. R. & Teufel, A. LASS6, an additional member of the longevity assurance gene family. *Int. J. Mol. Med.* **16**, 905–910 (2005).
- Ebel, P. et al. Inactivation of ceramide synthase 6 in mice results in an altered sphingolipid metabolism and behavioral abnormalities. *J. Biol. Chem.* **288**, 21433–21447 (2013).
- White-Gilbertson, S. et al. Ceramide synthase 6 modulates TRAIL sensitivity and nuclear translocation of active caspase-3 in colon cancer cells. *Oncogene* **28**, 1132–1141 (2009).
- Senkal, C. E., Ponnusamy, S., Bielawski, J., Hannun, Y. A. & Ogretmen, B. Anti-apoptotic roles of ceramide-synthase-6-generated C16-ceramide via selective regulation of the ATF6/CHOP arm of ER-stress-response pathways. *FASEB J.* **24**, 296–308 (2010).
- Hunger, S. P. & Mullighan, C. G. Acute lymphoblastic leukemia in children. *N. Engl. J. Med.* **373**, 1541–1552 (2015).
- Pui, C. H. & Evans, W. E. Treatment of acute lymphoblastic leukemia. *N. Engl. J. Med.* **354**, 166–178 (2006).
- Oltersdorf, T. et al. An inhibitor of Bcl-2 family proteins induces regression of solid tumours. *Nature* **435**, 677–681 (2005).
- Kang, M. H. & Reynolds, C. P. Bcl-2 inhibitors: targeting mitochondrial apoptotic pathways in cancer therapy. *Clin. Cancer Res.* **15**, 1126–1132 (2009).
- Chauhan, D. et al. A novel Bcl-2/Bcl-X(L)/Bcl-w inhibitor ABT-737 as therapy in multiple myeloma. *Oncogene* **26**, 2374–2380 (2007).
- Kang, M. H. et al. Activity of vincristine, L-ASP, and dexamethasone against acute lymphoblastic leukemia is enhanced by the BH3-mimetic ABT-737 in vitro and in vivo. *Blood* **110**, 2057–2066 (2007).
- Neale, G. et al. Molecular characterization of the pediatric preclinical testing panel. *Clin. Cancer Res.* **14**, 4572–4583 (2008).
- Holliday, M. W., Jr, Cox, S. B., Kang, M. H. & Maurer, B. J. C22:0- and C24:0-dihydroceramides confer mixed cytotoxicity in T-cell acute lymphoblastic leukemia cell lines. *PLoS One* **8**, e74768 (2013).
- Van Veldhoven, P. P. & Bell, R. M. Effect of harvesting methods, growth conditions and growth phase on diacylglycerol levels in cultured human adherent cells. *Biochim. Biophys. Acta* **959**, 185–196 (1988).
- Wang, X. et al. Mass spectrometric characterization of the affinity-purified human 26S proteasome complex. *Biochemistry* **46**, 3553–3565 (2007).
- Zhang, Y. et al. DSSylation, a novel protein modification targets proteins induced by oxidative stress, and facilitates their degradation in cells. *Protein Cell* **5**, 124–140 (2014).
- Kang, M. H. et al. National Cancer Institute pediatric preclinical testing program: model description for in vitro cytotoxicity testing. *Pediatr. Blood Cancer* **56**, 239–249 (2011).
- Kang, M. H., Wan, Z., Kang, Y. H., Spoto, R. & Reynolds, C. P. Mechanism of synergy of N-(4-hydroxyphenyl)retinamide and ABT-737 in acute lymphoblastic leukemia cell lines: Mcl-1 inactivation. *J. Natl. Cancer Inst.* **100**, 580–595 (2008).
- Makena, M. R., Koneru, B., Nguyen, T. H., Kang, M. H. & Reynolds, C. P. Reactive oxygen species-mediated synergism of fenretinide and romidepsin in preclinical models of T-cell lymphoid malignancies. *Mol. Cancer Ther.* **16**, 649–661 (2017).
- Morad, S. A. & Cabot, M. C. Ceramide-orchestrated signalling in cancer cells. *Nat. Rev. Cancer* **13**, 51–65 (2013).
- Kischkel, F. C. et al. Apo2L/TRAIL-dependent recruitment of endogenous FADD and caspase-8 to death receptors 4 and 5. *Immunity* **12**, 611–620 (2000).
- Kischkel, F. C. et al. Cytotoxicity-dependent APO-1 (Fas/CD95)-associated proteins form a death-inducing signaling complex (DISC) with the receptor. *EMBO J.* **14**, 5579–5588 (1995).
- Rossin, A. et al. Fas palmitoylation by the palmitoyl acyltransferase DHHC7 regulates Fas stability. *Cell Death Differ.* **22**, 643–653 (2015).
- Camgoz, A., Gencer, E. B., Ural, A. U., Avcu, F. & Baran, Y. Roles of ceramide synthase and ceramide clearance genes in nilotinib-induced cell death in chronic myeloid leukemia cells. *Leuk. Lymphoma* **52**, 1574–1584 (2011).
- Shakor, A. B. et al. Curcumin induces apoptosis of multidrug-resistant human leukemia HL60 cells by complex pathways leading to ceramide accumulation. *Biochim. Biophys. Acta* **1841**, 1672–1682 (2014).
- Schiffmann, S. et al. Ceramide synthases and ceramide levels are increased in breast cancer tissue. *Carcinogenesis* **30**, 745–752 (2009).
- Ruckhaberle, E. et al. Microarray analysis of altered sphingolipid metabolism reveals prognostic significance of sphingosine kinase 1 in breast cancer. *Breast Cancer Res. Treat.* **112**, 41–52 (2008).
- Suzuki, M. et al. Targeting ceramide synthase 6-dependent metastasis-prone phenotype in lung cancer cells. *J. Clin. Invest.* **126**, 254–265 (2016).

41. Karahatay, S. et al. Clinical relevance of ceramide metabolism in the pathogenesis of human head and neck squamous cell carcinoma (HNSCC): attenuation of C(18)-ceramide in HNSCC tumors correlates with lymphovascular invasion and nodal metastasis. *Cancer Lett.* **256**, 101–111 (2007).
42. Song, J. H., Kandasamy, K. & Kraft, A. S. ABT-737 induces expression of the death receptor 5 and sensitizes human cancer cells to TRAIL-induced apoptosis. *J. Biol. Chem.* **283**, 25003–25013 (2008).
43. Woo, M. et al. In vivo evidence that caspase-3 is required for Fas-mediated apoptosis of hepatocytes. *J. Immunol.* **163**, 4909–4916 (1999).
44. Jensen, S. A. et al. Bcl2L13 is a ceramide synthase inhibitor in glioblastoma. *Proc. Natl Acad. Sci. USA* **111**, 5682–5687 (2014).
45. Novgorodov, S. A. et al. SIRT3 deacetylates ceramide synthases: implications for mitochondrial dysfunction and brain injury. *J. Biol. Chem.* **291**, 1957–1973 (2016).